Cosolvent Effects on the Spontaneous Formation of Nanorod Vesicles in Catanionic Mixtures in the Rich Cationic Region

ARTICLE *in* THE JOURNAL OF PHYSICAL CHEMISTRY B · JUNE 2011

Impact Factor: 3.3 · DOI: 10.1021/jp202199d · Source: PubMed

5 AUTHORS, INCLUDING:

S. Javadian
Tarbiat Modares University
48 PUBLICATIONS **481** CITATIONS

SEE PROFILE

Hussein Gharibi
Tarbiat Modares University
68 PUBLICATIONS **1,347** CITATIONS

SEE PROFILE

THE JOURNAL OF PHYSICAL CHEMISTRY B

ARTICLE

pubs.acs.org/JPCB

Cosolvent Effects on the Spontaneous Formation of Nanorod Vesicles in Catanionic Mixtures in the Rich Cationic Region

Ali Yousefi, Soheila Javadian,* Hussein Gharibi, Jamal Kakemam, and Mohammad Rashidi-Alavijeh

Department of Physical Chemistry, Tarbiat Modares University, P.O. Box 14115-117, Tehran, Iran

Supporting Information

ABSTRACT: The aggregation behavior of cation-rich catanionic mixtures of cetyltrimethyl ammonium bromide (CTAB) and sodium dodecyl sulfate (SDS) was investigated in water−ethylene glycol (EG) solutions by performing surface tension, electrical conductivity, pulsed field gradient nuclear magnetic resonance, transmission electron microscopy, and cyclic voltammetry measurements. Different physicochemical properties such as the critical micelle concentration, degree of counterion dissociation (α), interfacial properties, aggregation numbers, morphology of aggregates, and interparticle interaction parameters were determined. Cosolvent effects on the interactions between the two surfactants CTAB and SDS were analyzed on the basis of regular solution theory, both for mixed monolayers at the air/liquid interface (β^{δ}) and for mixed micelles. It was shown that an excess of cationic surfactant resulted in the formation of nonspherical vesicles. These were predominantly nanorod vesicles in water−EG mixed solvents. The interparticle interactions were assessed in terms of cosolvent effects on the micellar surface charge density, the sphere-to-rod morphology change, and the phase transition from vesicles to mixed micelles. Moreover, the variation of the repulsive electrostatic potential energy between two pairs of aggregates was investigated for two modes of nanostructural transition, namely the transition between spherical and rod-like micelles and the transition between rod-like micelles and nanorod vesicles.

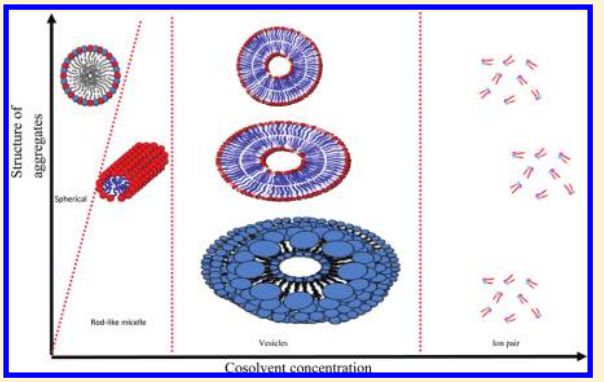

1. INTRODUCTION

Aqueous mixtures of anionic and cationic surfactants exhibit many unusual properties not possessed by other combinations of mixed surfactants. Catanionic (mixtures of cationic and anionic surfactants) mixtures of surfactants represent attractive systems for applications as they exhibit strongly synergistic interactions, which for instance lead to a large reduction in the critical micelle concentration (CMC).[1] The strongly attractive interactions between headgroups lead to a dramatic reduction in their areas, which allows the easy formation of aggregates, due to the changing packing parameter. Oppositely charged surfactants can form a wide variety of phases such as spherical micelles, rod-like micelles, disk vesicles, and lamellar liquid crystals, with the phase geometry depending on the strength of intermolecular interactions, the geometrical shape of the surfactants, the mole fraction of oppositely charged surfactants, concentration, and environmental factors (temperature, additives, etc). One of the noteworthy properties of systems of oppositely charged surfactants is their ability to spontaneously form vesicles.[1,2] In the past two decades many investigations have been carried out on various systems, most notably on the vesicular phase, since such systems can have major applications, for example in drug delivery, model membranes, microreactors, and cosmetics.[3]

Kaler et al. first reported the spontaneous formation of thermodynamically stable vesicles in cationic and anionic mixed-surfactant systems.[4] Prevost et al. investigated the aggregation behavior of two oppositely charged ionic surfactants (sodium dodecyl sulfate (SDS) and dodecyltrimethylammonium chloride (DTAC)) in aqueous media containing different added salts using small-angle neutron scattering (SANS).[3] The results showed that with no excess of salt, the nature of the counterion has no dominating effect on their aggregation behavior. Recently, catanionic micelles were studied in mixtures of cetyltrimethyl ammonium bromide (CTAB) and SDS by our group. Study of the variations in the self-diffusion coefficient and viscosity with changing concentration of CTAB or SDS in the cationic-rich and anionic-rich regions revealed a phase transition from microstructures (vesicles) to nanostructures (mixed micelles).[5] In an another work, we investigated the intermolecular interactions of SDS and CTAB in mixed monolayers and aggregates.[6] This investigation showed that the attractive interaction in mixed aggregates is weaker than in mixed monolayers at the air/solution interface. However, the results also showed that there is a strong synergism in these catanionic mixtures in both the aggregate and monolayer states. Further, temperature increases resulted in greater increases in the electrostatic attraction between the anionic groups

Received: March 8, 2011
Revised: May 15, 2011
Published: May 15, 2011

in anionic-rich mixtures compared to cationic-rich mixtures.[6] Several studies have been carried out on 1:1 (mol/mol) cationic/anionic surfactant mixtures, with surfactants including SDS-alkylprimaryammoniumchlorides,[7] SDS-alkyltrimethylammonium bromides,[8] and sodium alkylcarboxylates-alkyltrimethylammonium bromides,[9−11] with cosolvents (or solvents) including ethanol,[8−11] 1-propanol,[7−9] 2-propanol,[7−9] dimethyl sulfoxide,[9] formamide,[9] and 1-butanol.[9,12] The findings of these studies showed that the vesicle forming ability of mixed cationic and anionic surfactants can be improved by the addition of cosolvents to water. Yang et al[13,14] demonstrated that the stability of cationic vesicles is strongly depended on cosolvent addition. However, the effects of cosolvents on the formation of self-organized assemblies in cationic and anionic surfactant mixtures are not yet fully understood. Hence, the aim of the present work was to study the cosolvent effect on the behavior of cationic/anionic mixtures with an excess of cationic surfactant. We characterized the physicochemical properties and the morphology of these mixtures, and studied the ability of the systems to form vesicles. This research demonstrates, for the first time, the usefulness of cyclic voltammetry (CV) in studying the effects of varying solvent composition on interparticle interactions, sphere-to-rod geometry changes, and vesicle-to-micelle transitions.

2. EXPERIMENTAL SECTION

2.1. Materials. Hexadecyltrimethylammonium bromide (CTAB) and SDS were obtained from Merck. D_2O (99.9% purity) from Armar (Switzerland) was used as the solvent in NMR studies. Doubly distilled deionized water was used for sample preparation and dilution. Ethylene glycol (EG; Merck) was used for the preparation of stock solutions in pure water and EG-water mixed solvents. Samples were prepared by mixing the appropriate volumes of CTAB and SDS stock solutions. Mixed cationic−anionic surfactant systems precipitate easily in aqueous solutions because of strong interactions between them. To overcome this problem, our experiments are carried out in the rich cationic region. 2,2,6,6-Tetramethypiperidinl-1-oxy (TEMPO) and ferrocene (Merck) were also used without recrystallization.

2.2. Methods. *(a). Surface Tension Measurements.* Surface tension measurements were made with a Krüss K12 tensiometer under atmospheric pressure by the ring method.[15,16] The platinum ring was thoroughly cleaned and flame-dried before each measurement. The uncertainty of the measurements was ±0.1 mN/m. In all cases more than three successive measurements were carried out, and the standard deviation did not exceed 0.08 mN/m. A constant temperature was maintained by the circulation of thermostatted water through the jacketed vessel containing the solution. The temperature was controlled to within ±0.1 K.

(b). Electrical Conductivity Measurements. Conductivity measurements on the surfactant solutions were made using a conductometer (model Jenway 4510). After measuring the solvent conductivity, three successive measurements of the conductivity of the surfactant solutions were carried out (at constant temperature). The uncertainty of the measurements was ±0.01 μs.

(c). NMR Measurements. NMR self-diffusion studies were performed at room temperature using a Bruker 500 NMR spectrometer. A longitudinal eddy-current delay with a bipolar pulse pair (LEDBPP) pulse sequence[17] was used to determine the self-diffusion coefficients D.

(d). Cyclic Voltammetry Measurements. Cyclic voltammetry measurements were performed at 298 K using a SAMA 500 model, with electro-active probes of 2,2,6,6-tetramethylepiperidinyl-1-oxy(TEMPO) and ferrocene, an Ag/AgCl reference electrode, and platinum counter- and working electrodes. All solutions were prepared to a final volume of 25 mL, containing 0.1 mol dm^{-3} KCl, 0.001 mol dm^{-3} ferrocene, 0.002 mol dm^{-3} TEMPO, and different concentrations of surfactants. Due to the insolubility of ferrocene in water, ferrocene was first dissolved in ethanol before the small volume of the resulting ethanol solution was added to the aqueous surfactant solution. The small volume of the ethanol solution compared to the final solution volume meant that the effects of the ethanol were negligible. After every measurement, the surfaces of the working and counter electrodes were cleaned carefully by abrasion and washing with nitric acid.

(e). Transmission Electron Microscopy (TEM). Transmission electron micrographswere recorded on a Zeisselectron microscope (EM-10C) operated at 100 kV.

3. RESULTS AND DISCUSSION

3.1. Determination of the CMC and Interfacial Properties. The CMC values for different combinations of the binary CTAB/SDS mixture (in the cationic-rich regime) in aqueous mixtures of EG were determined from surface tension (Figure SM1) and conductivity (Figure SM2) plots, and are shown in Table 1. In addition, the CMC values for some binary combinations of the CTAB/SDS mixture were obtained using PFG-NMR in water (Figure SM3). It can be seen that a sharp fall in the CMC values for these binary combinations results from an increasing mole fraction of SDS (Table 1).

For pure CTAB and SDS, and 98:2 and 96:4 CTAB/SDS systems, surface tension, PFG-NMR and conductance measurements gave the same value for the CMC at 298 K in water (Table 1). There was no second CMC in this case. In the 92:8 CTAB/SDS system, surface tension and PFG-NMR measurements gave the same CMC values, but the CMC value obtained by conductance measurements was much higher. However, the γ- log C plot did show a dip at around the same value where there was a break in the conductance (see Figure 1). This break may be due to the formation of a second state of aggregation, which arises because of a change in the shape of the micelle. This shape change was evident in the data from CV measurements (Figure 2). For all of the combinations (in the cationic-rich regime) of the binary CTAB/SDS mixtures (except 98:2 CTAB/SDS systems in low volume fraction of EG (χ_{EG} = 0.1)), a second CMC was obtained.

It can be suggested that surface tension and PFG-NMR methods detect smaller micellar aggregates formed at lower concentrations. However, the conductance method is capable of detecting large micellar aggregates resulting from sphere-to-rod transitions. This suggests that CMC determination also depends on the micelle size, which is surprising. Overall, it can be inferred that surface tension and PFG-NMR methods give an accurate estimate of micelle formation, and hence the CMC. The first CMC corresponds to the formation of normal spherical micellar aggregates by the association of surfactant monomers at a critical concentration, whereas the second state of aggregation represented by the second CMC is due to structural transformations at surfactant concentrations well above the first CMC. Such micellar transitions for catanionic surfactant systems have been reported by our group[5,6] and other researchers.[13,18] Moreover,

Table 1. Critical Micelle Concentration and Degree of Counter Ion Dissociation, α, and Surface Parameters of Mixed Micellization of CTAB/SDS in Water−EG Solutions at 298 K

α_{CTAB}	$10^3 \times$ CMC[a] (mol dm^{-3})	$10^3 \times$ CMC[b] (mol dm^{-3})	α_{diss}	$10^6 \times \Gamma_{max}$ (molecule m^{-2})	A_{exp} (nm^2 molecule^{-1})	A_{idea} (nm^2 molecule^{-1})	Π_{cmc} (mN m^{-1})
				$\chi_{EG} = 0$			
1	1.10	1.05	0.23	2.88	0.57		39.72
0.98	0.92 (1.00[d])	0.98 (0.94[c])	0.28	2.84	0.58	0.57	35.78
0.96	0.83	0.95	0.31	2.89	0.68	0.56	39.19
0.94	0.39	0.92	0.33	2.90	0.57	0.56	42.45
0.92	0.21 (0.12[c], 0.30[d])	0.90 (0.91[c])	0.37	2.80	0.59	0.56	40.87
0	8.10	8.50	0.33	3.01	0.55		35.70
				$\chi_{EG} = 0.1$			
1	1.13	1.20	0.30	2.84	0.58		35.81
0.98	0.97	1.10	0.31	2.86	0.58	0.58	35.02
0.96	0.93	0.98	0.37	2.43	0.57	0.58	36.74
0.94	0.43	0.94	0.38	2.41	0.68	0.58	30.23
0.92	0.36	0.89	0.40	2.60	0.63	0.58	31.43
0	8.70	8.60	0.38	2.91	0.57		30.56
				$\chi_{EG} = 0.2$			
1	1.40	1.46	0.35	2.38	0.69		30.69
0.98	0.40	1.44	0.39	2.10	0.79	0.67	32.73
0.96	0.29	1.42	0.39	2.04	0.65	0.67	30.83
0.94	0.26	1.36	0.38	2.14	0.77	0.67	30.86
0.92	0.21	1.32	0.41	2.06	0.80	0.67	31.51
0	9.20	9.30	0.42	2.66	0.62		26.48
				$\chi_{EG} = 0.35$			
1	2.10	2.3	0.41	1.48	1.12		25.23
0.98	0.43			2.07	0.87	1.04	26.76
0.96	0.34			1.40	1.18	1.03	24.28
0.94	0.24			0.91	1.82	1.02	25.75
0.92	0.22			0.81	2.05	1.02	27.09
0	9.8	11	0.47	1.92	0.86		22.54
				$\chi_{EG} = 0.5$			
1	2.90			1.36	1.22		23.68
0.98	0.17			1.41	1.18	1.30	20.52
0.96	0.018			1.30	1.28	1.29	12.87
0.94							
0.92							
0	15.40			1.22	1.36		21.02

[a] The values obtained from surface tension measurements. [b] The values obtained from conductometry measurements. [c] The values in parentheses obtained from CV measurements. [d] The values in parentheses obtained from PFG-NMR method.

the presence of a second CMC was suggested for other systems such as TTAB(tetradecyl trimethylammonium bromide)/Brij-35-(polyoxyethylene (23) lauryl ether),[19] C_nTAB/TX-100(*tert*-octyl phenyl polyoxyethylene ether),[20,21] C_nTAB(n = 10,12)/C_mTAB(m = 14,16),[22] cationic dimeric (gemini)/nonionic surfactants,[23] and SDS/cpc(cetyl pyridinium chloride).[24,25] For TTAB/Brij-35 mixed surfactant systems, sphere-to-rod transitions and the formation of two different kinds of micelles by the constituent surfactants were considered as possible reasons for the second state of aggregation.[19] In the latter case, one kind of micelle would be a mixed micelle containing both TTAB and Brij-35 in a single micelle, while the other would be micelles formed from only one surfactant type (i.e., pure TTAB and pure Brij-35 micelles).[19] In C_nTAB/TX-100, two different kinds of micelle (rich- nonionic and rich-cationic surfactant micelles) formed.[19,20]

Figure 2 shows the variation of i_p upon increasing the total surfactant concentration for 98:2 and 92:8 CTAB/SDS mixtures. Initially, the addition of small quantities of surfactant mixtures resulted in a small decrease in the i_p value, due to very weak interactions between the electroactive probe and the monomeric surfactant.[26,27] These interactions are understood to be a result of the weak hydrophobic environment available for the solubilization of the probe. A further increase in the surfactant concentration leads to micelle formation, which facilitates the solubilization of electroactive probe. The TEMPO in the micellar phase instantaneously reduces i_p, which therefore tends to a negligible constant value. CMC values were obtained from a plot of i_p versus total surfactant concentration (Table 1). These values agreed with the tensiometry and PFG-NMR results. In CV measurements, the addition of supporting electrolyte does not

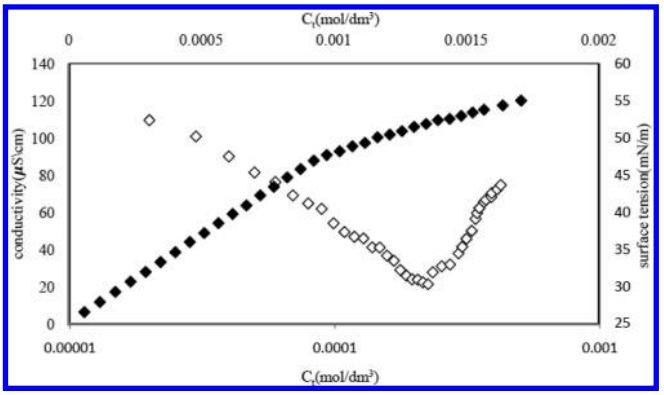

Figure 1. Effect of the total concentration on the specific conductivity and surface tension in water + EG solutions (χ_{EG} = 0.1) at 298 K: ♦, conductivity; ◊, surface tension. A solution molar relation of CTAB/SDS of 92:8 is considered.

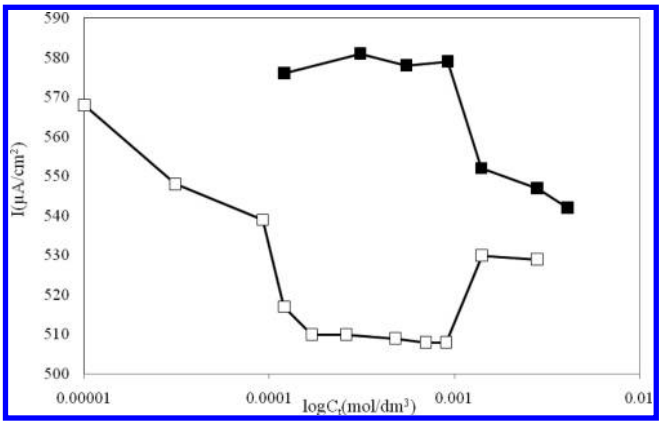

Figure 2. Plot of peak current vs total concentration for mixtures of CTAB and SDS in aqueous solutions at 298 K: ■, 98:2 CTAB/SDS; □, 92:8 CTAB/SDS.

significantly change the CMC values. These results are in agreement with previous findings.[3] For the 92:8 CTAB/SDS mixtures, two discontinuities in the i_p versus concentration plot were observed. These discontinuities correspond to the first and second CMCs of this system. These results suggest that primary micelles can aggregate so as to form secondary micelles.

Cyclic voltammograms for the one-electron oxidation of TEMPO in CTAB/SDS at various scan rates for the potential range 0.0−1.0 V are given in Figure SM 4a.

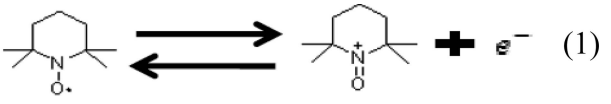

(1)

In CV, the peak current i_{pa} for a redox-active reversible system is given by the Randles-Sevcik equation[28]

$$i_{pa} = 0.4463FACn\left(\frac{nF\nu D}{RT}\right)^{1/2} \quad (2)$$

where n is the number of electrons involved in oxidation or reduction, A is the area of the electrode (A was determined by the method described in the Supporting Materials (SM1)), F is Faraday's constant, R is the gas constant, T is the absolute temperature, D is the diffusion coefficient of the TEMPO probe, C is the concentration of TEMPO in the solution, and ν is the scan rate. In the case where the probe is distributed between the micelles and the bulk phase (it can be assumed that the peak currents of the free probe and micellar probe are independent), it can be shown using eq 2 that

$$D^{1/2} = \frac{i_{pa}}{0.4463F^{3/2}ACn^{3/2}R^{-1}T^{-1}\nu^{1/2}} = \frac{D_m{}^{1/2}KN_{agg}{}^{-1}(C - CMC) + D_f{}^{1/2}}{1 + KN_{agg}{}^{-1}(C - CMC)} \quad (3)$$

where D is the observed diffusion coefficient in the micellar system and D_f and D_m are the TEMPO diffusion coefficients in the bulk and micelle phases respectively. The micelle self-diffusion is monitored based on the cyclic voltammograms for the one- electron oxidation of ferrocene, which can be assumed to be completely solubilized in the micellar phase (next section). The solution of eq 3 yielded the partition coefficient (K) of TEMPO between the bulk and micellar phases. It was found that the K value is about 3995 ± 395 and 3226 ± 850 M^{-1} for 92:8 and 98:2 CTAB/SDS respectively in the first CMC region. The K values decrease to 491 ± 95 M^{-1} in the second CMC region for 92:8 CTAB/SDS systems, due to a decrease in the solubility of the TEMPO. This reduction in solubility may be ascribed to the altering morphology of aggregates. Consistent with the present results, previous studies have noted that the probe is sensitive to the surfactant concentration, and can mirror the changes taking place within the structure of the aggregates.[29] It is not possible to perform CV measurements for CTAB/SDS mixtures in water−EG solutions. This is due to an overlap in the cyclic voltammograms for EG and TEMPO.

The degrees of counterion dissociation (α_{diss}, measured using conductometry) at various volume fractions of EG are listed in Table 1 for CTAB, SDS, and different CTAB/SDS cationic-rich mixtures. These results show that the degree of counterion dissociation for the pure surfactants and their mixtures increases monotonically with increasing volume fraction of EG. The observed increases in α_{diss} are probably due to decreases in the charge density at the micellar surface, resulting from decreases in the aggregation number in the pure micelles. The value of α_{diss} is higher in CTAB/SDS mixtures than in pure CTAB systems (Table 1). This suggests a reduction of the charge density at the micellar surface due to the presence of SDS in the micelles.

Previously, we explained the influence of increasing the EG content in the solution on the CMC and α_{diss} by considering dielectric effects in the medium.[30] The addition of EG affects both the interactions between hydrophobic groups and the interactions between hydrophilic groups in the surfactants. The dielectric constant of EG is much lower than that of water, and so the addition of EG into water will make the dielectric constant of the mixed solvent lower. Therefore, on the one hand the addition of EG into aqueous solutions renders the hydrophobic effect of the catanionic surfactant molecules weaker, which is a disadvantage for micelle formation. On the other hand, the addition of EG strengthens the attractive electrostatic interaction between their two oppositely charged polar groups, and consequently is an advantage for micelle formation. In CTAB/SDS mixtures, this overcomes the disadvantageous influence of EG addition on the hydrophobic effect. It can be seen that the presence of EG in the bulk phase affects the micellization process of CTAB/SDS

mixtures, leading to more spontaneous micellization, while in pure CTAB and SDS systems an increase in the volume fraction of EG causes the micellization process to occur less spontaneously. This can be understood on the basis of a reduction in the solvophobic interactions caused by the improved solvation in the presence of EG, which leads to an increase in the solubility of the hydrocarbon tails and electrostatic repulsion between head groups (in ionic systems),which results in an increase in the CMC.

An effective measure of the adsorption of surfactant at the air−liquid interface is usually obtained by the surface excess concentration, Γ_{max}, which can be determined by the Gibbs equation for dilute solutions.[31]

$$\Gamma_{max} = \frac{-1}{2.303nRT}\left[\frac{d\gamma}{d\log C}\right]_{T,P} \quad (4)$$

Here R and T are respectively the gas constant and temperature, γ is the surface tension, C is the concentration of surfactant, and n is the number of species formed in solution considering the dissociation per monomer. The minimum area per headgroup (A_{min}) for surfactant molecules at the CMC at the saturated interface was obtained by the following equation:[31]

$$A_{min} = \frac{10^{18}}{N_A\Gamma_{max}}(nm^2/molecule) \quad (5)$$

where N_A is Avogadro's number. Γ_{max} was calculated using a curve fitted to a plot of γ versus log C. The fit was performed using a polynomial equation (PE) $y = ax^2 + bx + C$, and Γ_{max} was then calculated by determining the slope of the tangent at the CMC.[32] The R^2 (regression coefficient) value of the fit was between 0.9 and 0.99. Table 1 shows that the values of Γ_{max} for CTAB/SDS mixtures do not change significantly with increasing amounts of EG until higher concentrations of EG are reached. The observed (and expected) decrease in Γ_{max} can be attributed to several factors, including (1) a change in the water structure due to the addition of EG, (2) the interaction between EG and the surfactant, and(3) the presence of EG at the interface.[16] As expected, A_{min} demonstrates an inverse trend with respect to Γ_{max}, since the amount of EG is increased (Table 1). Furthermore, the low value of A_{min} in pure water and at low percentages of EG in the mixed solution suggests that the air/liquid interface is closely packed, and therefore the surfactant molecules at the interface are oriented almost perpendicular to the interface. Table 1 shows the ideal mixing values, A_{ideal}, calculated from the equation $A_{ideal} = Z_1A_1 + (1 - Z_1)A_2$, where Z_1 is the mole fraction of component 1 in the mixed monolayer, and A_1 and A_2 designate the minimum area per molecule of CTAB and SDS, respectively. This is true, except for some cases, in which the experimental A_{min} values are greater than A_{ideal}, inspite of the strong synergism between them. It is possible that there is some van der Waals self-attraction between the hydrophobic portions of each CTAB molecule before mixing, which is reduced upon mixing with SDS.

3.2. Surfactant−Surfactant Interactions in the Aggregated Phase and in Monolayers at the Liquid−Air Interface. The nature and the strength of the interactions between two surfactants in binary systems can be determined by calculating their β parameters, which can be achieved using the regular solution model developed by Rubingh et al.[33−35]

Table 2. Cosolvent Effect on β^M_{ave} and β^σ_{ave} Values

χ_{EG}	β^M_{ave}	β^δ_{ave}	$\beta^\delta_{ave} - \beta^M_{ave}$
0.0	−7.86	−8.26	−0.4
0.1	−6.92	−5.80	1.12
0.2	−11.91	−12.70	−0.79
0.35	−13.26	−15.35	−2.09
0.5	−22.35	−24.62	−2.27

The interaction parameter for mixed micelle in an aqueous medium, β^M is calculated using the following equations:[36]

$$\frac{(X_1^M)^2\ln(\alpha_1 C_{12}^M/X_1C_1^M)}{(1-X_1^M)^2\ln[(1-\alpha_1)C_{12}^M/(1-X_1^M)C_2^M]} = 1 \quad (6)$$

$$\beta^M = \frac{\ln[\alpha_1 C_{12}^M/X_1C_1^M]}{(1-X_1^M)^2} \quad (7)$$

where X_1^M is the mole fraction of surfactant 1 in the mixed surfactant solution and C_1^M, C_2^M, and C_{12}^M are the CMCs for surfactant 1, surfactant 2, and their mixture, respectively, at the mole fraction α_1.

The interaction parameter for mixed monolayer at the aqueous solution/air interface, β^σ, is calculated using the following equations:[37−39]

$$\frac{Z_1^2\ln(\alpha_1 C_{12}/Z_1C_1^0)}{(1-Z_1)^2\ln[(1-\alpha_1)C_{12}/(1-Z_1)C_2^0]} = 1 \quad (8)$$

$$\beta^\sigma = \frac{\ln(\alpha_1 C_{12}/Z_1C_1^0)}{(1-Z_1)^2} \quad (9)$$

Here Z_1 is the mole fraction of surfactant 1 in the total mixed monolayer (on a surfactant-only basis); and C_1^0, C_2^0, and C_{12} are the molar concentrations in the solution phases of surfactant 1, surfactant 2, and their mixture, respectively, at the mole fraction α_1 of surfactant 1 required to produce a given γ value. In our experiments, we determined C_1, C_2, and C_{12}, which correspond to a surface tension of $\sigma = 38.5$ mN m^{-1} (see Figure 1). Equation 8 is solved numerically for Z_1, which is then substituted into eq 9 to calculate β^σ.

According to the Rubingh model, the interaction parameter calculated through eqs 1 and 2 should be independent of micellar composition. However, the application of this model yields a composition-dependent interaction parameter, β^M (supporting materials). The obtained values of β^M_{ave} are listed in Table 2. The $|\beta^M_{ave}|$ value provides information on the strength of the degree of interaction between two surfactants, and is related to the degree of nonideality of this interaction in mixed micelles. Large negative values of β^M indicate a strong attractive interaction between CTAB and SDS. According to the data in Table 2, with increasing EG content in the aqueous solution, $|\beta^M_{ave}|$ decreases slightly; this can be attributed to the structure-breaking nature of EG in water and a reduction in the hydrophobic interactions, and these are the main driving forces for mixed micellization. On the other hand, $|\beta^M_{ave}|$ increases at higher vol. percentages of EG. The increase in $|\beta^M_{ave}|$ values at higher vol. percentages of EG can be mainly attributed to the increase in electrostatic attraction between the two oppositely charged, polar, ionic head groups of CTAB and SDS upon mixing. It is interesting to note that there is a close comparison between the trend in the $|\beta^M_{ave}|$ values

obtained here (with increasing EG content for CTAB/SDS)and results reported for ionic/nonionic[30] mixtures. We observed that the value of $|\beta^{M}_{ave}|$ decreases slightly up to 10% EG, but then increases sharply with further increases in EG. As shown in Table 2, there is a similar trend between $|\beta^{M}_{ave}|$ and $|\beta^{\sigma}_{ave}|$ with addition of EG. As shown in Table 2, the interaction parameter $|\beta^{\sigma}_{ave}|$ goes through a minimum as the vol. percentage of EG in solution is increased from 0% to 50%. The initial decrease in $|\beta^{\sigma}_{ave}|$ as EG is added to aqueous solution is attributed to a reduction in the attractive van der Waals interactions between hydrophobic groups at the planar air/aqueous solution, due to the structure-breaking nature of EG in water and the presence of EG in the monolayer at the air/aqueous solution interface. The increase in $|\beta^{\sigma}_{ave}|$ at higher vol. percentages of EG could result from increases in the electrostatic attraction between ionic hydrophilic groups through mixing. Furthermore, it is shown that the value of $\beta^{\sigma}_{ave} - \beta^{M}_{ave}$ at first increases with increasing EG concentration (up to 10%), reaches a maximum at a specific concentration, and thereafter decrease with further increasing EG concentration (Table 2). This suggests that the increase in electrostatic attraction between the two oppositely charged, polar head groups (of CTAB and SDS) resulting from the increased amount of EG (≫10%) in the aqueous medium has a greater effect at the planar air/aqueous interface than at the convex micellar surface in an aqueous medium. In short, the present results indicate that greater electrostatic attraction energy is generated at the planar interface than in the micelle.

3.3. Size, Morphology and Interactions of Catanionic Self-Assemblies. CV measurements were used to determine the diffusion coefficients of the mixed aggregates and the interparticle interaction parameters.[40] For this section, ferrocene was chosen as the electroactive probe; ferrocene can be used provided that it does not perturb the micelle, and provided that its rates of entrance/exit into the aggregates with fast and reversible electron transfer are at least comparable to those of the surfactant monomers. The electrochemistry of ferrocene in nonaqueous, aqueous, and micellar environments is described elsewhere.[41−45]

The cyclic voltammograms for the one-electron oxidation of ferrocene (eq 10) in CTAB/SDS mixtures at various scan rates for the potential range 0.0−0.5 V are given in Figure SM5b.

$$Fc \leftrightarrows Fc^{+} + e^{-} \qquad (10)$$

For self-assembly systems involving an electroactive probe completely solubilized in the aggregates, D in eq 2 corresponds to the aggregate diffusion coefficient D_{agg}, since the probe diffuses with the aggregates. Hence, from the slope of the i_{pa} versus $v^{1/2}$ plot, the D_{agg} values were obtained for various mixed aggregate concentrations; the concentration of ferrocene was fixed at 1×10^{-3} mol/L. D_{agg} was found to decrease with increasing surfactant concentration for all CTAB/SDS mixtures in water−EG solutions (Figure 3). In the CV measurements, it is possible that the addition of supporting electrolyte influenced D_{agg}. According to previous studies, the salt concentration has no dominant effect on the morphology and properties in a mixture of oppositely charged surfactants.[3] Therefore we expect no significant change in the morphology of catanionic self-assemblies with the addition of salt.

At concentrations above but not far from the CMC, aggregates mutually interact; consequently, the calculated values for the diffusion coefficients are lower than those at the CMC. As attenuation of the mass-transport parameters is a linear function

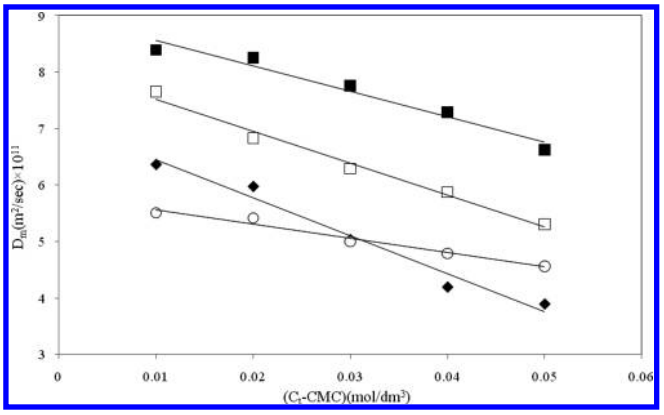

Figure 3. Self-diffusion coefficient, D_m as a function of total concentration of surfactants for 92:8 CTAB/SDS mixtures in water−EG solutions at 298 K: ■, χ_{EG} = 0; □, χ_{EG} = 0.1; ○, χ_{EG} = 0.2; ♦, χ_{EG} = 0.35.

Table 3. Value of k_d (dm^3 mol^{-1}) and Aggregation Numbers (N_{agg}) for CTAB/SDS Mixed Aggregates in Water−EG Solutions at 298 K

	χ_{EG} = 0		χ_{EG} = 0.1		χ_{EG} = 0.2		χ_{EG} = 0.35	
CTAB/SDS	k_d	N_{agg}	k_d	N_{agg}	k_d	N_{agg}	k_d	N_{agg}
98:2	5.7		5.7		8.5		11.1	
96:4	5.1		6.6		8.5		11.1	
94:6	4.3		7.0		8.6		10.8	
92:8	3.3	1331	7.5	4195	8.7	18248	10.0	

of surfactant concentration, linear interaction theory was used for the calculation of interparticle interaction parameters.[46,47] Consequently, extrapolation to infinite dilution (i.e., to the CMC) yields mass-transport parameters that are independent of interparticle interactions.

$$D_{agg} = D^{0}_{agg}[1 - k_d(C_t - CMC)] \qquad (11)$$

where k_d is the interparticle interaction parameter, D^{0}_{agg} is the self-diffusion coefficient in the absence of particle interaction, and C_t is the surfactant concentration. The dependence of the self-diffusion coefficient on aggregate concentration is shown in Figure 3. We propose that the dependence of D_{agg} on surfactant concentrations depends on both repulsive and attractive interactions, micellar growth, and phase transitions. However, our experiments were carried out in a concentration range where micellar growth and phase transitions are negligible. As can be seen from eq 11, the slope is given by $D^{0}_{m}k_d$ and the intercept is given by D^{0}_{m}, so by dividing the slope by the intercept the interparticle interaction parameter k_d is directly obtained from the curve. The k_d and D^{0}_{agg} values are summarized in Table 3. It can be seen that the k_d values are influenced by the increasing mole fraction of anionic surfactant in the studied solutions (Table 3). The repulsive interactions between mixed aggregates are gradually reduced with the addition of anionic surfactant, resulting in the decrease in k_d observed for these mixed systems in water. The mole fractions of SDS (X_{SDS}) and CTAB (X_{CTAB}) in aggregates, obtained using a regular solution model (Table SM1), confirmed the decrease in micellar charge density. The variation of k_d from 5.7 to 3.3 dm^3 mol^{-1} with increasing SDS

dx.doi.org/10.1021/jp202199d |J. Phys. Chem. B 2011, 115, 8112–8121

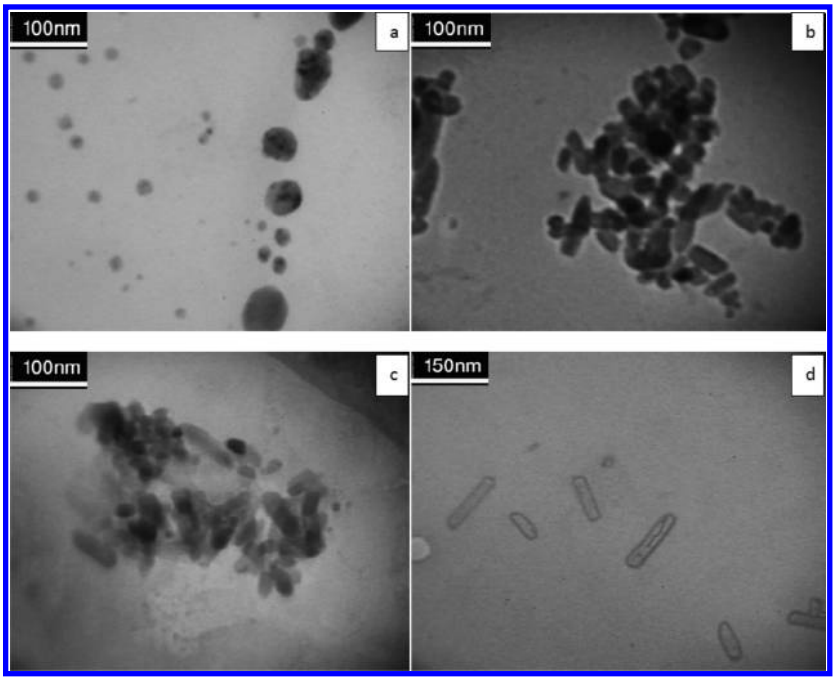

Figure 4. TEM photographs of CTAB/SDS mixtures at (a) 98:2 (X_{EG} = 0.1, after 12 h), (b) 92:8 (X_{EG} = 0.1, after 12 h), (c) 98:2 (X_{EG} = 0.2, after 12 h), and (d) 92:8 (X_{EG} = 0.2, after 12 h).

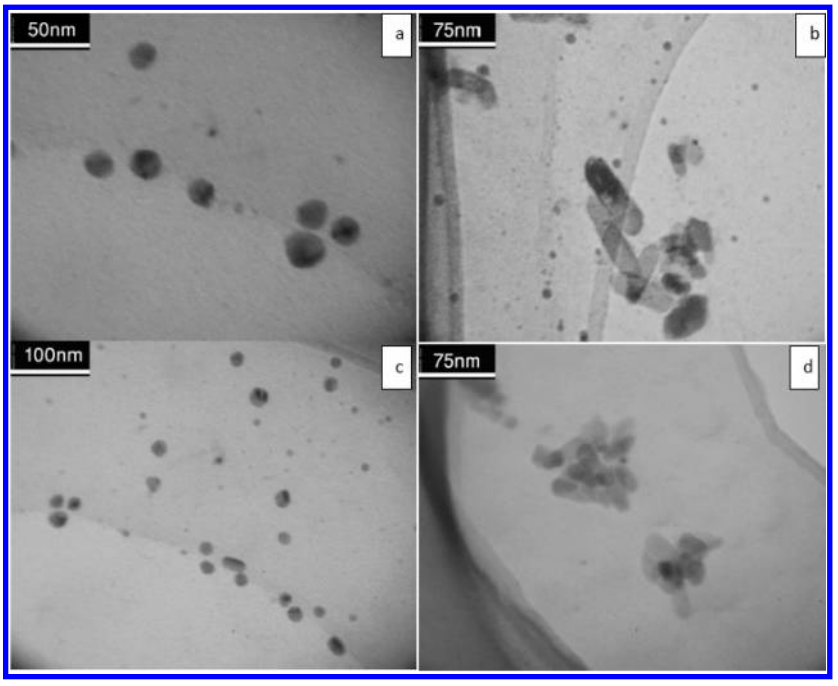

Figure 5. TEM photographies of CTAB/SDS mixtures at (a) 92:8 (X_{EG} = 0, after 12 h), (b) 92:8 (X_{EG} = 0, after 1 month), (c) 98:2 (X_{EG} = 0.1, after 12 h), and (d) 98:2 (X_{EG} = 0.1, after 1 month).

mole fraction indicated that the linear spherical expansion of micelles becomes predominant. The CTAB/SDS micellar structures remained spherical in the cationic region, and no dramatic structural changes took place in the solutions. As shown in Figure 4, TEM images confirmed the results of the CV studies. In pure water and 92:8 CTAB/SDS, we can see that 3−60 nm polydisperse spherical micelles are formed (Figure 6). Also, Sarkar et al showed that spherical micelles formed at a higher concentration of CTAB(concentration of SDS = 0.03 mM and concentration of CTAB = 10 mM).[48] It is reasonable to suggest that the surfactant composition is not a key factor in determining the shape, size and polydispersity of aggregates.

As shown in Table 3, increasing the EG content in the aqueous solution to 10% resulted in no significant change in k_d for the 98:2 CTAB/SDS systems. These results were confirmed by TEM characterization (Figure 4). In addition, the surface tension

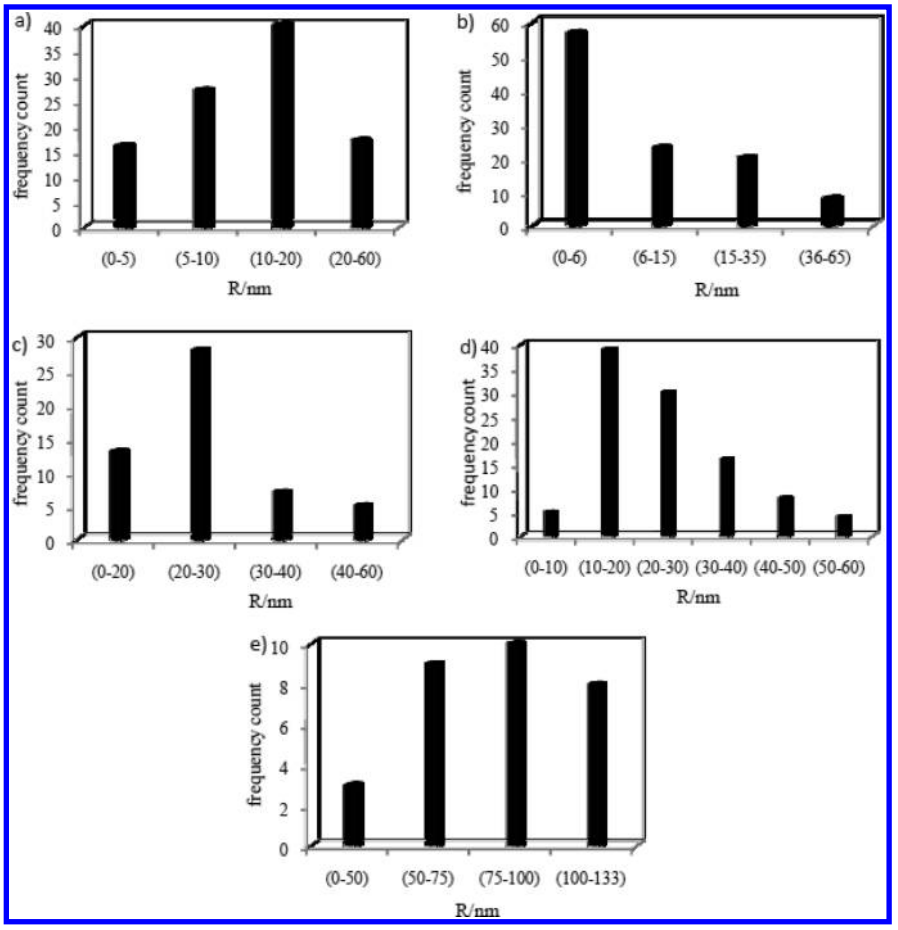

Figure 6. Size distribution plots of mixed aggregates: (a) 92:8 (X_{EG} = 0, after 12 h), (b) 92:8 (X_{EG} = 0, after 1 month), (c) 98:2 (X_{EG} = 0.1, after 1 month), (d) 92:8 (X_{EG} = 0.1, after 12 h), and (e) 92:8 (X_{EG} = 0.2, after 12 h).

and conductometry studies validated the finding that the addition of 10% EG did not perturb these systems (Table 1). However, in the presence of 10% EG the CTAB/SDS systems (except the 98:2 CTAB/SDS system) did not display behavior similar to that shown by CTAB/SDS in pure water. As shown in Table 3, the k_d values for the CTAB/SDS systems increased monotonically with increasing anionic surfactant mole fraction in the presence of 10% EG. In spite of the decrease in micellar surface charge density with addition of SDS (Table SM 1), an increase in k_d values was observed. This unexpected increase in k_d values can be mainly attributed to the spherical-to-cylindrical morphology change. Representative TEM photographs of 92:8 CTAB/SDS mixed micelles at 10% EG confirmed the above results (Figure 4). The average length of the cylindrical structures in Figure 4 is ~20−30 nm. In both the case of pure water and in 10% EG−water solutions, the addition of anionic surfactant reduces headgroup−headgroup repulsion and causes micellar growth. On the other hand, in 10% EG solutions the addition of EG causes a phase transition from spherical to cylindrical structures. The polydispersity slightly decreased with increasing EG (Figure 4). Moreover, we observed a phase transition from spherical to cylindrical structures after one month for 92:8 CTAB/SDS in pure water and 98:2 CTAB/SDS in 10% EG in water (Figure 5). With further addition of EG, the k_d values increased to approximately 8 and 11 $dm^3\ mol^{-1}$ in 20% and 35% EG solutions, respectively, and were unchanged with increasing SDS content. The increase in k_d values may be due to a phase transition from micelles to vesicles. The observed lack of variation of k_d indicates that the morphology does not change significantly with increasing SDS mole fraction. TEM imaging confirmed the morphology of aggregates in a 20% EG solution for 98:2 and 92:8 CTAB/SDS systems (Figure 4). For 98:2 CTAB/SDS, spherical vesicles, nonspherical vesicles, and cylindrical vesicles were observed, and the system was more polydispersed (Figures 4 and 6). With the further addition of SDS the monodispersity of the system increased, and 50−150 nm cylindrical vesicles or nanorod vesicles formed (Figures 4 and 6). The further addition of EG into water decreases the dielectric constant of the mixed solvent. Therefore, the magnitude of the surfactant tail transfer free energy and the hydrophobic interactions of catanionic surfactant molecules are decreased, which are disadvantages in regards to the energy requirement for vesicle formation. On the other hand, the attractive electrostatic interaction between the two oppositely charged polar groups is increased, leading to an increase in the free energy, which are advantages in regards to the energy requirement for vesicle formation. In suitable cases, this effect may overcome the disadvantageous influence of EG addition on hydrophobic interactions, resulting in more favorable energy conditions for vesicle formation. Our previous studies showed that, over a narrow range of surfactant mixing ratios CTAB/SDS ≈ 0.66−0.77 (molar ratio of CTAB), vesicles are the only stable aggregate structure,[5] whereas with the addition of EG to solutions the vesicles are formed over a wide range of ratios of CTAB/SDS,

particularly in the rich cationic region. Most researchers have reported on vesicle formation in 1:1anionic/cationic surfactant mixtures in cosolvent−water mixtures.[13] In this work, we focused on the cationic-rich regime and discussed the findings in detail. In addition, as a new approach, we stressed the potential significance of intermicellar interaction parameters in the quantitative interpretation of micellar growth, change in morphology and micelle-vesicle transitions. The aggregation numbers were calculated using the method described in SM2. As shown in Table 3, the aggregation numbers increased remarkably with the addition of EG, which confirmed the strong synergism in cat-anionic systems.

To further examine the observed behavior, the interparticle interaction energy (Coulombic potential) between two identical charged particles was calculated (for both spherical and cylindrical particles).[49]

The intermicellar interaction energy (Coulombic potential) for two spherical macro-ions of diameter σ was calculated as[50,51]

$$U(r) = U_0 a \exp[-\kappa(r-a)]/r$$
$$U_0 = \frac{z^2 e^2}{4\pi\varepsilon\varepsilon_0 a(2+\kappa a)^2} \quad (12)$$

where r is the micellar center-to-center distance, ε is the dielectric constant of the medium (H_2O), ε_0 is the permittivity of free space, κ is the Debye−Huckle inverse screening length as determined from the ionic strength of the solution, and $a = 2R_h^0$, where R_h^0 is the aggregate hydrodynamic radius. R_h^0 can be obtained from TEM images. The value for r can be calculated from the aggregate volume fraction (φ) (obtained from R_h^0) as follows:

$$r = 2R_h^0 + 1 \quad (13)$$

$$l^3 = [8\pi/2^{1/3}]\varphi(R_h^0)^3 \quad (14)$$

For two cylindrical charged particles, the interparticle interaction energy can be calculated in the two spatial cases where the particles are either parallel or crossed[49,52−54]

$$U_{cy}^{\parallel}(H) = \frac{2\sqrt{\pi a}\sigma^2}{\varepsilon_r\varepsilon_0\kappa^{3/2}} Li_{1/2}(e^{-\kappa H}) \quad (14)$$

$$U_{cy}^{\perp}(H) = \frac{4\pi a\sigma^2}{\varepsilon_r\varepsilon_0\kappa^2} \ln\left(\frac{1}{1-e^{-\kappa H}}\right) \quad (15)$$

where H is the distance between two cylinders, a is radius of the core of the cylinder, σ is the amount fixed charge contained in the surface layer per unit area, and $Li_s(Z)$ is the polylogarithm function, defined by

$$Li_s(z) = \sum_{k=1}^{\infty} \frac{z^k}{k^5} \quad (16)$$

From the potential distribution, the repulsive potential energy can be obtained for cylindrical charged particles.

Figure 7 shows the variation of $U(r)$ with H and l in water-EG solutions. As shown in Figure 7, the electrostatic repulsion interaction between aggregates increased due to two modes of nanostructural transition; the transition between spherical and rodlike micelles and the transition between rodlike micelles and nanorod vesicles.

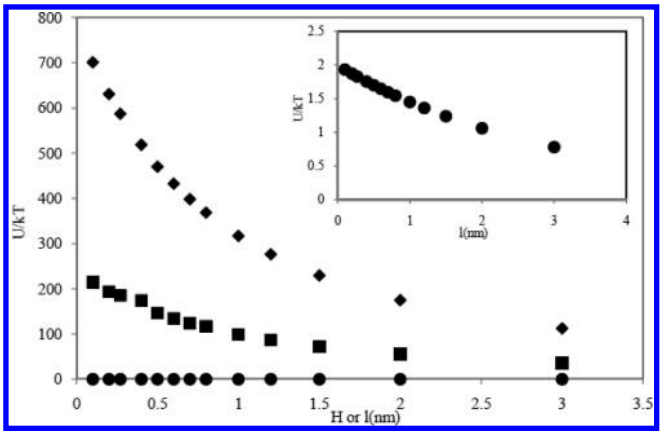

Figure 7. Plot of $U(r)/KT$ versus H or l for 92:8 CTAB/SDS systems in water−EG solutions: ●, χ_{EG} = 0; ■, χ_{EG} = 0.1; ♦, χ_{EG} = 0.2.

4. CONCLUSION

A binary composition of SDS/CTAB with an excess of cationic surfactant produced two CMC values in water−EG mixed solvents (except in solutions of 98:2 CTAB/SDS in 10% EG in water). To consider the effects of cosolvents on the surfactant−surfactant interaction in binary anionic/cationic surfactants, the values of β parameters were calculated. It was shown that adding EG to the solution reduces the magnitude of the interaction parameters in both mixed micelle (β^M) and mixed monolayer (β^σ) This indicates a greater effect on the interaction in the mixed monolayer in comparison with mixed micelle. At a higher volume fraction of EG, the synergism effect of mixed aggregates is increased significantly which is contributed from the increase in attractive electrostatic interaction between oppositely charged head groups upon mixing.

This study has demonstrated that the percentage of cosolvent variation is an effective method of tuning intra-aggregate interaction and inducing a micelle−vesicle transition or morphology change in catanionic systems. As a new approach, we stressed the potential significance of intermicellar interaction parameters in the quantitative interpretation of micellar growth, change in morphology and micelle−vesicle transitions. The intermicellar interaction parameter values increased due to change morphology and a phase transition from micelles to vesicles.

■ ASSOCIATED CONTENT

Supporting Information. Additional plots of experimental data, equations, references and a table. This material is available free of charge via the Internet at http://pubs.acs.org.

■ AUTHOR INFORMATION

Corresponding Author

*E-mail: javadians@yahoo.com; javadian_s@modares.ac.ir. Fax: +98 − 21-82883755.

■ REFERENCES

(1) Tsuchiya, K.; Jshikake, J.; Kim, T. S.; Ohkubo, T.; Sakia, H.; Abe, M. *J. Colloid Interface Sci.* **2007**, *312*, 139–145.

(2) Singh, K.; Marangoni, D. G.; Quinn, J. G.; Singer, R. D. *J. Colloid Interface Sci.* **2009**, *335*, 105–111.

(3) Prevost, S.; Gradzielski, M. *J. Colloid Interface Sci.* **2009**, *337*, 427–484.

(4) Kaler, E. W.; Murthy, A. K.; Rodriguez, J. A. N. *Science* **1989**, *245*, 1371–1374.
(5) Sohrabi, B.; Gharibi, H.; Javadian, S.; Hashemianzadeh, M. *J. Phys. Chem. B* **2007**, *111*, 10069–10078.
(6) Sohrabi, B.; Gharibi, H.; Tajik, B.; Javadian, S.; Hashemianzadeh, M. *J. Phys. Chem. B* **2008**, *112*, 14869–14876.
(7) Zhang, X. R.; Huang, J. B.; Mao, M.; Tang, S. H.; Zhu, B. *Y. Colloid Polym. Sci.* **2001**, *279*, 1245–1249.
(8) Wang, C. Z.; Tang, S. H.; Huang, J. B.; Zhang, X. R.; Fu, H. *L. Colloid Polym. Sci.* **2002**, *280*, 770–774.
(9) Huang, J. B.; Zhao, B. Y.; Mao, M.; He, P.; Wang, J.; He, *X. Colloid Polym. Sci.* **1999**, *277*, 354–360.
(10) Huang, J. B.; Zhu, B. Y.; Zhao, G. X.; Zhang, Z. Y. *Langmuir* **1997**, *13*, 5759–5761.
(11) Huang, J. B.; Zhao, G. X. *Colloid Polym. Sci.* **1995**, *273*, 156–164.
(12) Marques, E. F.; Regev, O.; Khan, A.; Lindman, B. *Adv. Colloid Interface Sci.* **2003**, *100-102*, 83–104and references therein.
(13) Yu, W. Y.; Yang, Y.-M.; Chang, C. H. *Langmuir* **2005**, *21*, 6185–6193.
(14) Yeh, S. J.; Yang, Y.-M.; Cang, C. H. *Langmuir* **2005**, *21*, 6179–6184.
(15) Rodriguez, M. A.; Munos, M.; Graciani, M. M.; Pachon, M. S. F.; Moya, M. L. *Colloids Surf. A: Physicochem. Eng* **2007**, *298*, 177.
(16) Ruiz, C. C.; Molina-Boliver, J. A.; Aguiar, J.; Macisaac, G.; Moroze, S.; Palepu, R. *Langmuir* **2001**, *17*, 6831.
(17) Wu, D. H.; Chen, A. D.; Johnson, C. S. *J. Magn. Reson.* **1995**, *115*, 260.
(18) Yatcill, M. T. Y.; Herrington, K. L.; Brasher, L. L.; Kaler, E. W. *J. Phys. Chem.* **1996**, *100*, 5874–5879.
(19) Sharama, K. S.; Patil, S. R.; Rakshit, A. K. *J. Phys. Chem. B* **2004**, *108*, 12804–12812.
(20) Gharibi, H.; Javadian, S.; Hashemianzadeh, M. *Colloids Surf. A: Physicochem. Eng.* **2004**, *323*, 77–86.
(21) Gharibi, H.; Sohrabi, B.; Javadian, S.; Hashemianzadeh, *M. Colloids Surf., A* **2004**, *244*, 187–196.
(22) Ray, G. B.; Chkraborty, I.; Ghosh, S.; Moulik, S. P.; Palepu, *R. Langmuir* **2005**, *21*, 10958–10967.
(23) Wang, Y.; Marques, E. F. *J. Mol. Liquids* **2008**, *142*, 136–142.
(24) Chakraborty, T.; Ghosh, S.; Moulik, S. P. *J. Phys. Chem. B* **2005**, *109*, 14813–14823.
(25) Maiti, K.; Bhattacharya, S. C.; Moulik, S. P.; Panda, A. *K. Colloids Surf., A* **2010**, *355*, 88–98.
(26) Mahajan, R. K.; Kaur, N.; Bakshi, M. S. *Colloids Surf., A* **2006**, *276*, 221–227.
(27) Mahajan, R. K.; Vohra, K. K.; Shaheen, A.; Aswal, V. K. *J. Colloid Interface Sci.* **2008**, *326*, 89–95.
(28) Chokshi, K.; Qutubuddin, S.; Hussam, A. *J. Colloid Interface Sci.* **1989**, *129*, 315.
(29) Mandal, A. B.; Balachandran, U. N.; Ramasswamy, D. *Langmuir* **1988**, *4*, 736–739.
(30) Javadian, S.; Gharibi, H.; Fallah, H. T. *J. Chem. Eng. Data* **2010**, *55*, 1122–1130.
(31) Rosen, M. J. *Surfactants and Interfacial phenomena*, 3rd ed.; John Wiley: New York, 2004.
(32) Sharma, K. S.; Rodgers, C.; Palepu, R.; Rakshit, A. K. *J. Colloid Interface Sci.* **2003**, *268*, 482.
(33) Holland, P. M.; Rubhing, D. N. *J. Phys. Chem.* **1983**, *87*, 1984.
(34) Holland, P. M.; Rubhing, D. N. *J. Colloid Interface Sci.* **1993**, *158*, 258.
(35) Schulz, P. C.; Rodriguez, J. L.; Minardi, R. M.; Sierra, M. B.; Morini, M. A. *J. Colloid Interface Sci.* **2006**, 303.
(36) Bai, G.; Wang, J.; Yan, H.; Li, Z.; Thomas, R. K. *J. Phys. Chem. B* **2001**, *105*, 3105.
(37) Wang, Y.; Marques, E. F. *J. Mol. Liq.* **2008**, *142*, 136–142.
(38) Zhou, Q.; Rosen, M. J. *Langmuir* **2003**, *19*, 4555–4562.
(39) Rosen, M. J.; Zhou, Q. *Langmuir* **2001**, *17*, 3532–3537.
(40) Geetha, B.; Mandal, A. *Langmuir* **1997**, *13*, 2410–2413.
(41) Charlton, I. D.; Doherty, A. P. *J. Phys. Chem. B* **2000**, *104*, 8327–8332.
(42) Ferreira, T. L.; Sato, B. M.; Elseoud, O. A.; Bertotti, M. *J. Phys. Chem. B* **2009**, *114*, 857–862.
(43) Charlton, I. D.; Doherty, A. P. *Colloids Surf., A* **2001**, *182*, 305–310.
(44) Charlton, I. D.; Doherty, A. P. *Langmuir* **1999**, *15*, 5251–5256.
(45) Chen, Z. X.; Deng, S. P.; Li, X. K. *J. Colloid Interface Sci.* **2008**, *318*, 389–396.
(46) Dickinson, E. *Ann. Rep. Prog. Chem. Sec. C: Phys. Chem.* **1983**, *80*, 3–37.
(47) Mandal, A. B. *Langmuir* **1993**, *9*, 1932–1933.
(48) Sarkar, M.; Chkraborty, H. *Langmuir* **2004**, *20*, 3551–3558.
(49) Ohshima, H.; Hyono, A. *J. Colloid Interface Sci.* **2009**, *333*, 202–208.
(50) Zhenyu Yang, Y. L.; Jinsheng, Z.; Qingato, G.; Xiuli, Y.; Zhengyu, Y. *J. Phys. Chem. B* **2004**, *108*, 7523–7527.
(51) Ikeda, S. *Colloid Polym. Sci.* **1991**, *269*, 49.
(52) Ohshima, H. *Colloid Polym. Sci.* **1996**, *274*, 1176–1182.
(53) Hayter, J.; Penford, B. *J. Mol. Phys.* **1981**, *42*, 109–118.
(54) Juyoung, C.; Hyunbae, D.; Seungjoo, H.; Sang-yup, L. *Bull. Korean Chem. Soc.* **2008**, *29*, 1131.